Indian Journal of Fundamental and Applied Life Sciences ISSN: 2231– 6345 (Online)
An Open Access, Online International Journal Available at www.cibtech.org/sp.ed/jls/2015/04/jls.htm
2015 Vol. 5 (S4), pp. 969-977/Aghaei
Research Article

FINITE ELEMENT ANALYSIS OF HELMET SUBJECTED TO BULLET IMPACT

***Mohammad Aghaei Asl**
Department of Civil Engineering, Payame Noor University, Iran
**Author for Correspondence*

ABSTRACT
Helmet has been used as protective equipment in order to shield human head from impact-induced injuries such as in traffic accident, sports, construction work, military, factory and some other human activities. The helmets attempt to guard the wearer's head through mechanical energy absorbing process. Hence, the structure and protective capacity of the helmets are altered in high energy impact. The purpose of this project was (1) to study how different combat helmet shell stiffness affects the load levels in the human head during a bullet impact, and (2) to study how different impact angles affects the load levels in the human head. A detailed finite element (FE) model of the human head, in combination with an FE model of a combat helmet (the US Personal Armor System Ground Troops' (PASGT) geometry) was used. Focus was aimed on getting a realistic response of the coupling between the helmet and the head and not on modeling the helmet in detail. The studied data from the FE simulations were stress in the cranial bone, strain in the brain tissue, pressure in the brain, change in rotational velocity and translational and rotational acceleration. A parametric study was performed to see the influence of a variation in helmet shell stiffness on the outputs from the model. The effect of different impact angles was also studied. Dynamic helmet shell deflections larger than the initial distance between the shell and the skull should be avoided in order to protect the head from the most injurious threat levels. It is more likely that a fracture of the skull bone occurs if the inside of the helmet shell strikes the skull. Oblique ballistic impacts may in some cases cause higher strains in the brain tissue than pure radial ones.

Keywords: *Combat Helmet; Finite Element; Head Injuries; Impact Angel; Brain Tissue*

INTRODUCTION
Historically, the helmet used by the soldiers was reintroduced during World War I by General Adrian of the French army. General Adrian had made 700,000 metal caps (calotte) and were able to defeat 60% of the metal-fragment hits and saved his soldiers from severe head wound (Gawande, 2004). The development of the army helmet was continued with the introduction of M-1 helmet by the American troops during the outbreak of World War II, Korean War and Vietnam War. It consists of steel outer shell and inner liner shell made of cotton fabric-reinforced phenolic laminate (Warden, 2008). The PASGT was fielded in 1982 and first used in Grenada 1983.

Figure 1: U.S helmet and interior Pad system

© Copyright 2014 | Centre for Info Bio Technology (CIBTech)

The shell was made of Kevlar 29 fibers reinforced with resin and molded under heat and pressure. The helmet came with five sizes and weight in the range of 1.31 kg to 1.9 kg. The bulge ear section was to provide the space for communications equipment. The retention-suspension system, fixed on the shell, was made of nylon webbing in the form of basket to provide a stable helmet-head interface. The standoff distance between the head and the helmet was 12.3mm, thus it allowed for ventilation and heat transfer as well as transient deformation due to ballistic impact (Carey *et al.*, 2000). Figure 1 shows U.S helmet and materials interior Pad system.

MATERIAL AND METHODS

FE Model of Combat Helmet and Bullet

To model the elastic response of the helmet and padding, we used the Neo-Hookean model extended to the compressible range, in which the strain energy density is given by:

$$W(C) = \frac{\lambda}{2} log^2 J - \frac{\mu}{2}(I_1 - 3) \quad (1)$$

where μ and λ are Lame constants and I_1 is the first invariant of the right Cauchy-Green deformation tensor C. Standard material properties for Helmet/padding: Density=1440 (kg/m^3), E=1.24e9 (Pa), ν=0.36.

Figure 2 shows three views of a shell model of a helmet with the FE mesh and Contact interfaces; dimensions are in mm. The bounding surfaces of the helmet are traction free except for the two nodes marked in red which are constrained from moving in all three directions.

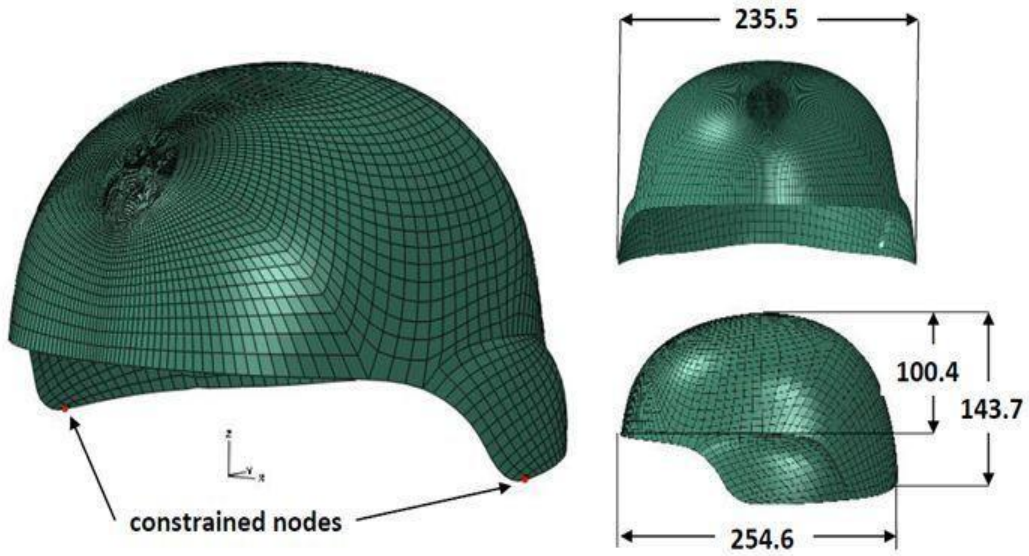

Figure 2: FE model of combat helmet

Once the modeling, meshing and material property assignments were completed, the next step is to assemble the various finite element models for simulation. The rationale and purpose behind each test scenario will be explained in detail.

As mentioned before, there are two ballistic test standards and the test conditions will be applied to all scenarios depending on whether the projectile used is the FMJ or the FSP. The FMJ for example will have a striking velocity of 358m/s and the FSP a striking velocity of 610m/s. These two ballistic test standards were tested against the helmet in actual experimental conditions. The task is to replicate these actual conditions in the form of simulations and with the validation of the result; it is then possible to predict other events that are ballistic related impacts (Figure 3).

© Copyright 2014 | Centre for Info Bio Technology (CIBTech)

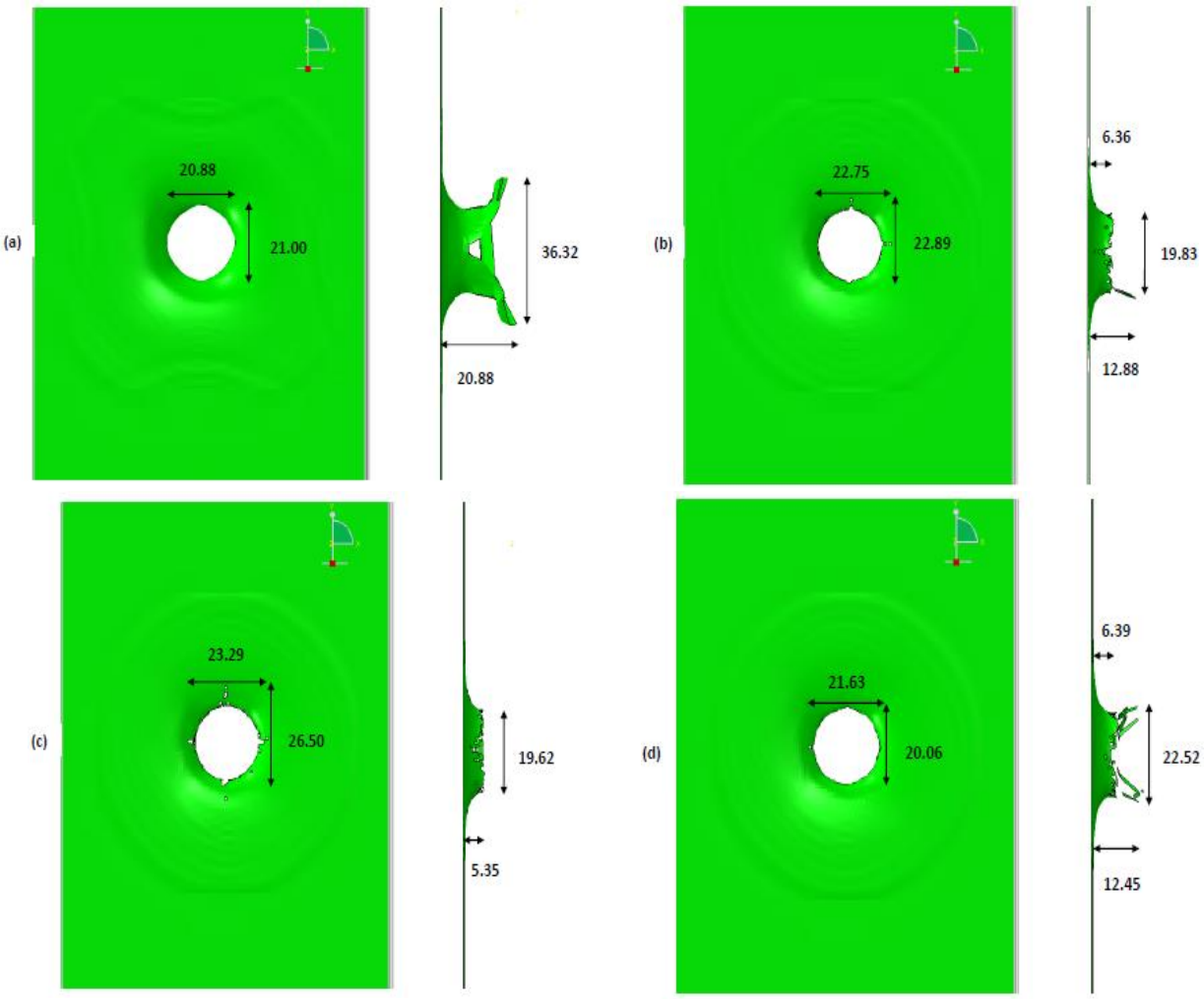

Figure 3: Front and side views of the five composite laminates after penetration by the projectile; AS4/3501-6 (a), E-glass/117-220 (b), Gevetex/LY556 (c), Silenka/MY750 (d); all dimensions in mm

Using the principle of conservation of energy, the energy balance during the impact simulations appears as (neglecting the potential energy):

$$KE_{bullet} = KE_{helmet+head+bullet} + IE_{helmet+head} + WF \quad (2)$$

where KE is kinetic energy, IE is internal energy and WF is the work of friction in the contact interfaces. The hourglass energy was below 5% in all simulations and considered insignificant for the illustration of the energy distribution.

Brain-tissue Materials Model

Various numbers of head components have been modeled by the deferent authors. The head is modeled with Lagrangian elements and directly from the design (CAD 3D) drawings (Figure 4).

The image data are segmented into 3 different tissue types of the head: (1) skull, (2) cerebrospinal fluid (CSF) and (3) brain. The brain is surrounded by ca. 140ml of CSF. This fluid cushions the brain from mechanical shock and, during normal movement, shrinking and expansion of the brain is quickly balanced by an increase or decrease of CSF that can flow from the cranial cavity into the spinal cavity through the foramen magnum. The skull and CSF are modeled as linear, elastic, isotropic materials with properties adopted from the literature (Sarron *et al.,* 2000; Helms *et al.,* 2007). Hrapko (2008) presented an overview of available literature on the material properties of brain tissue. Brain tissue can generally be defined as a heterogeneous, viscoelastic solid, consisting for up to 80% of water.

© Copyright 2014 | Centre for Info Bio Technology (CIBTech)

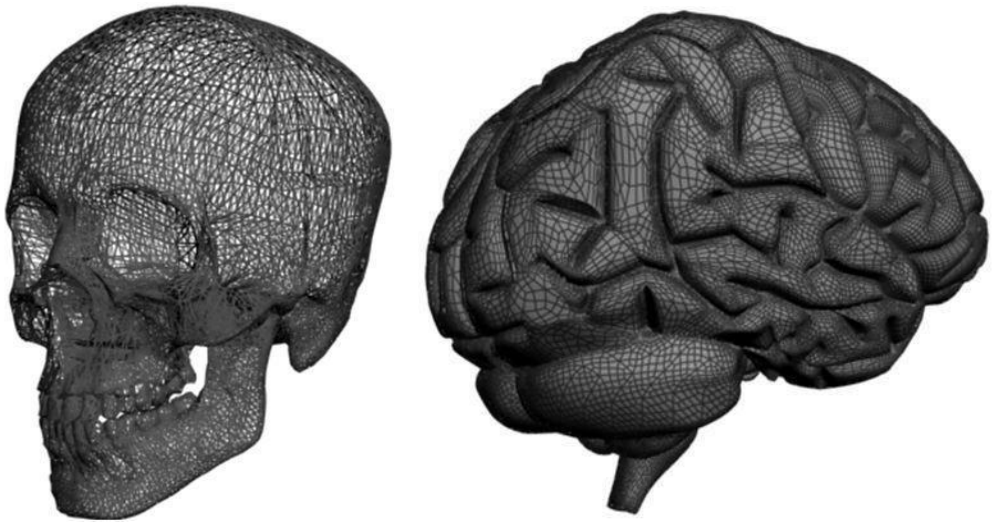

Figure 4: FE model of the human head

The material is almost incompressible (Poisons ratio ν~0.5), and can be assumed to only deform in shear (Brands, 2002). The brain is modeled with an elastic volumetric response and viscoelastic shear response. The material data used in this study are taken from the literature and listed in Tables 1.

Table 1: The material data used for modeling

Elastic material properties of the skull and CSF layer

Tissue	**Density** ρ **(kg/m^3)**	**Young's modulus** E **(Pa)**	**Poisson's ratio** (υ)
Skull	2070	6.5E+9	0.20
CSF	1004	1.5E+5	0.49886

Viscoelastic material properties of the brain

Tissue	**Density** ρ **(kg/m^3)**	**Bulk modulus** K **(Pa)**	**Short-term shear modulus** G_0 **(Pa)**	**Long-term shear modulus** G_∞ **(Pa)**	**decay constant** β **(s^{-1})**
Grey matter	1040	2.19E+9	3.4E+4	6.4E+3	400
White matter	1040	2.19E+9	4.1E+4	7.8E+3	400

In this study, we use a material model which assumes linear viscoelastic, isotropic behavior for both grey and white matter. The standard linear solid model is applied to characterize the shear behavior, and the shear relaxation modulus is described by:

$$G(t) = G_\infty + (G_0 - G_\infty)e^{-\beta t} \quad (3)$$

where G_0 is the short-term shear modulus, G_∞ is the long-term shear modulus, and β is a decay constant. The material parameters used are the same as those in Zhang *et al.*, (2004). The interface between all these tissue types are modeled as tied contact. The bottom of the neck is constrained in all six degrees of freedom to avoid rigid body motion.

RESULTS AND DISCUSSION

Results

To analyze the effect of different helmet shell stiffness's on the load levels in the human head, the material properties of the shell were altered within realistic limits. Six different shell stiffness's were modeled, generating a maximum deflection of the inside of the helmet shell of 12.5, 15.0, 20.0, 25.0, 30.0 and 35.0 mm, respectively, in radial impacts. For simplification these shell configurations are hereafter called A, B, C, D, E and F, respectively. A represents the stiffest shell while F represents the most

© Copyright 2014 | Centre for Info Bio Technology (CIBTech)

compliant shell. The material properties presented by van Hoof *et al.*, (2001) were scaled according to Table 2 to create these different shell properties. $E_1 = E_2 = 18.5$ GPa, $E_3 = 6.0$ GPa, (1–3 being the principal material directions), $\nu_{12} = 0.25$, $\nu_{13} = \nu_{23} = 0.33$, $\rho = 1.23$ g/cm^3.

Table 2: Material data for the different shell configurations (Aare M and Kleiven S, 2007).

Shell configuration	Deflection (mm)	G12 (GPa)	G13/G23 (GPa)	S1/S2 (MPa)	S3 (MPa)	S12 (MPa)	S13/S23 (MPa)
A	12.5	0.77	2.72	555.0	1200.0	77.0	1086.0
B	15.0	0.39	2.44	277.5	600.0	38.5	543.0
C	20.0	0.25	0.90	183.2	396.0	25.4	358.4
D	25.0	0.19	0.68	138.8	300.0	19.3	271.5
E	30.0	0.15	0.54	111.0	240.0	15.4	217.2
F	35.0	0.12	0.41	83.3	180.0	11.6	162.9

G—shear modulus; S—strength values; 1–3—principal material directions

It is clear that the stress in the cranial bone increases remarkably when a contact between the shell and the skull is initiated. Also, the pressure span in the brain increases for the most compliant helmet shell. When looking at strains in the brain tissue there is an optimum, and the helmet shell should neither be neither too stiff nor too compliant (Table 3).

Table 3: Results from the parametric study on the helmet shell stiffness.

	Helmet shell configuration					
	A	**B**	**C**	**D**	**E**	**F**
Impact angle (90° is pure radial)	90	90	90	90	90	90
Contact between helmet shell and skull	NO	NO	NO	YES	YES	YES
Max. von Mises stress in the compact skull bone (Mpa)	32	33	36	85	110	160
Max. von Mises stress in the cancellous skull bone (Mpa)	4.1	3.9	4.8	12	17	22
Max. pressure in the brain (Mpa)	0.47	0.43	0.37	0.33	0.41	0.54
Min. pressure in the brain (Mpa)	-0.34	-0.34	-0.31	-0.35	-0.34	-0.55
Max. principal strain in the white brain tissue	0.14	0.14	0.13	0.09	0.10	0.11
Max. principal strain in cortex	0.14	0.15	0.13	0.09	0.10	0.11
Max. principal strain in corpus callosum	0.09	0.08	0.05	0.06	0.05	0.05
Max. principal strain in the brain stem	0.09	0.09	0.08	0.07	0.07	0.08
Translational acceleration of the head (g)	83	89	89	102	119	138
Rotational acceleration of the head (krad/s^2)	2.1	2.1	3.2	3.8	2.6	1.9
Rotational velocity change (rad/s)	2.2	1.8	2.3	3.5	2.0	1.8

Table 4: Results from the study on different impact angles.

	Impact angle (90° is pure radial)			
	22.5	**45**	**67.5**	**90**
Helmet shell configuration	D	D	D	D
Contact between helmet shell and skull	NO	YES	YES	YES
Max. von Mises stress in the compact skull bone (Mpa)	20	32	69	85
Max. von Mises stress in the cancellous skull bone (Mpa)	2.2	3.8	9.6	12
Max. pressure in the brain (Mpa)	0.29	0.28	0.33	0.33
Min. pressure in the brain (Mpa)	- 0.27	-0.33	-0.35	-0.35
Max. principal strain in the white brain tissue	0.10	0.17	0.11	0.09
Max. principal strain in cortex	0.10	0.16	0.12	0.09
Max. principal strain in corpus callosum	0.04	0.07	0.05	0.06
Max. principal strain in the brain stem	0.06	0.08	0.08	0.06
Translational acceleration of the head (g)	46	83	96	102
Rotational acceleration of the head (krad/s^2)	4.6	7.0	2.8	3.8
Rotational velocity change (rad/s)	4.4	6.6	3.4	3.5

© Copyright 2014 | Centre for Info Bio Technology (CIBTech)

The stress in the cranial bone increases with the impact angle. Also, the pressure in the brain shows a small dependence on the impact angle. It is obvious that an impact angle of 45° cause's higher strains in the brain than the other impact angles (Table 4).
A larger angle significantly reduces the maximum v-m stress on skull bone, which is shown in Figure 5, as well as the absolute values of the maximum/minimum pressure and maximum principal strain in the brain tissue.

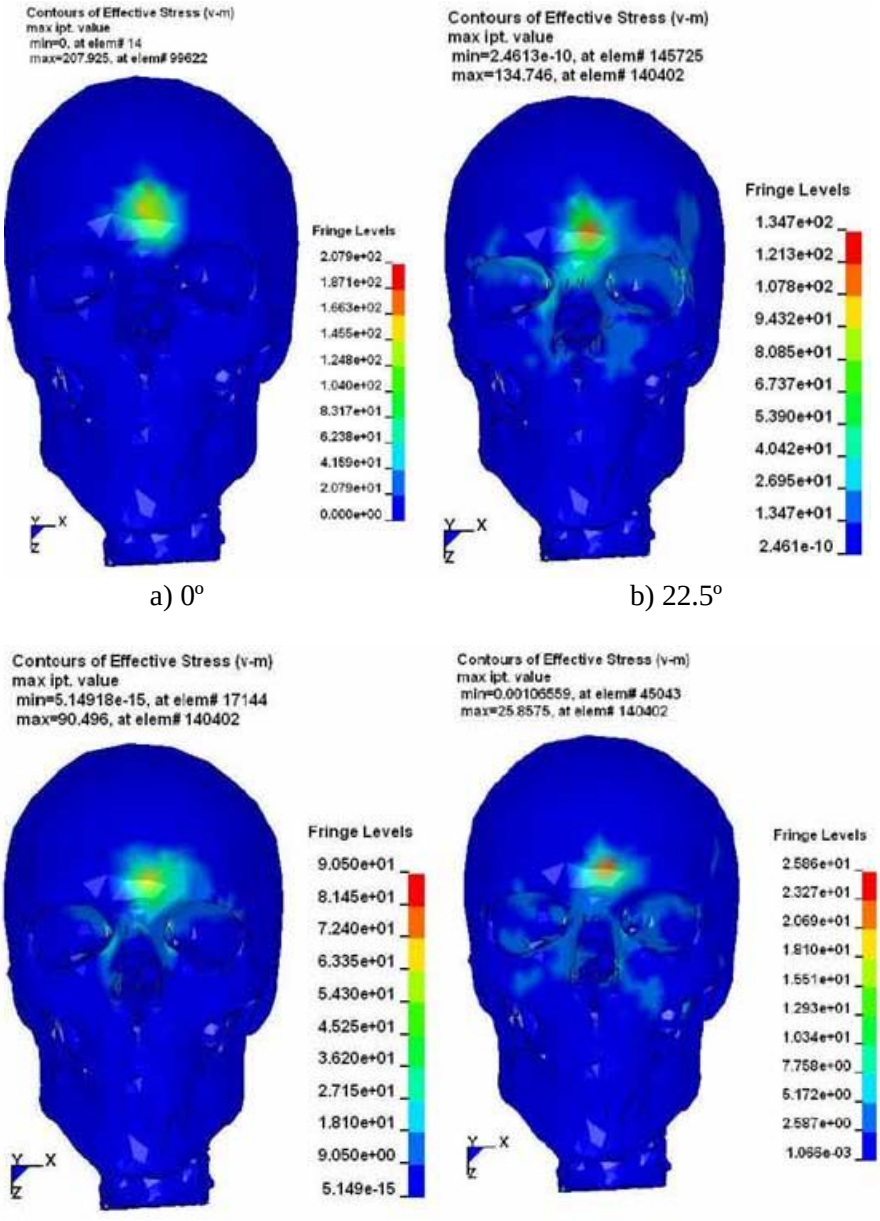

a) 0º b) 22.5º

a) 45º b) 67.5º

Figure 5: The Von Mises stress distributions on skull when the bullet is hits the helmet with different impact angles.

The failed elements during a simulation could be visualized in Figure 6. The size of the region having failed elements increased with decreasing material stiffness and strength. For the most compliant shell, a typical delaminating behavior, with a separation of the solid layers, could be seen during the simulation.

© Copyright 2014 | Centre for Info Bio Technology (CIBTech)

This zone was much smaller for the stiffer helmet shells. The simulation using the shell stiffness configuration, E, showed similar maximal deflection to the ones seen in the shooting tests of aramide laminate helmets. It should, however, be noted that the composite material model might not be well-suited to describe the yield and failure of titanium.

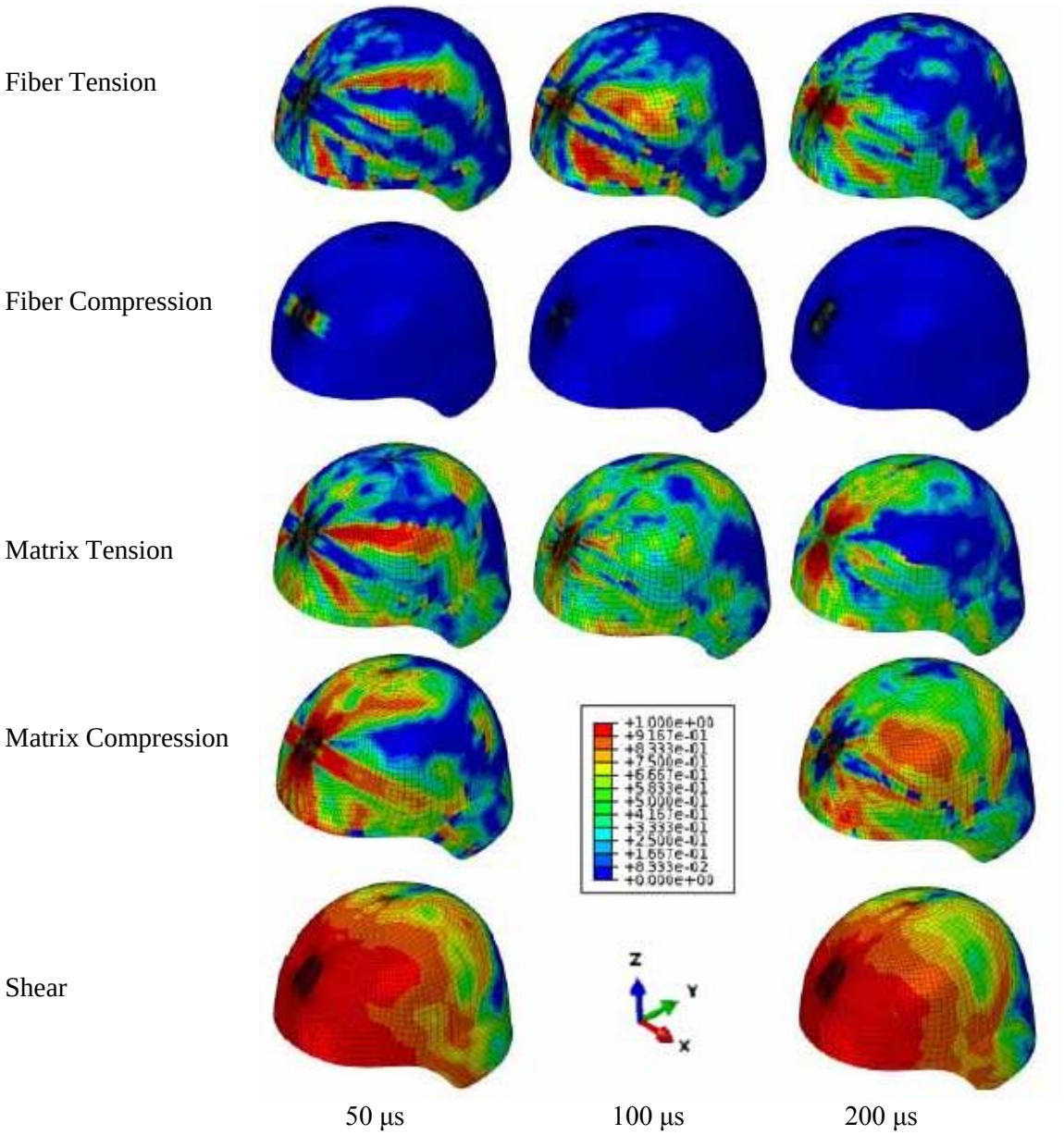

Figure 6: Visualization of failed elements during simulation

One of the most commonly used criterions for predicting head injuries is the head injury criterion (HIC). The formula is taken from literature (Prasad P and Mertz HJ, 1985), and the equation is:

$$HIC = \left[\frac{1}{(t_2-t_1)}\int_{t_1}^{t_2} a(t)\right]^{2.5}(t_2 - t_1) \quad (4)$$

In which $a(t)$ denotes the translational head acceleration in g's as a function of time, and t_1 and t_2 represent the initial and final times of an interval that maximizes this function. Figure 7 and 8 illustrates HIC for 90° frontal and side impact.

© *Copyright 2014 | Centre for Info Bio Technology (CIBTech)*

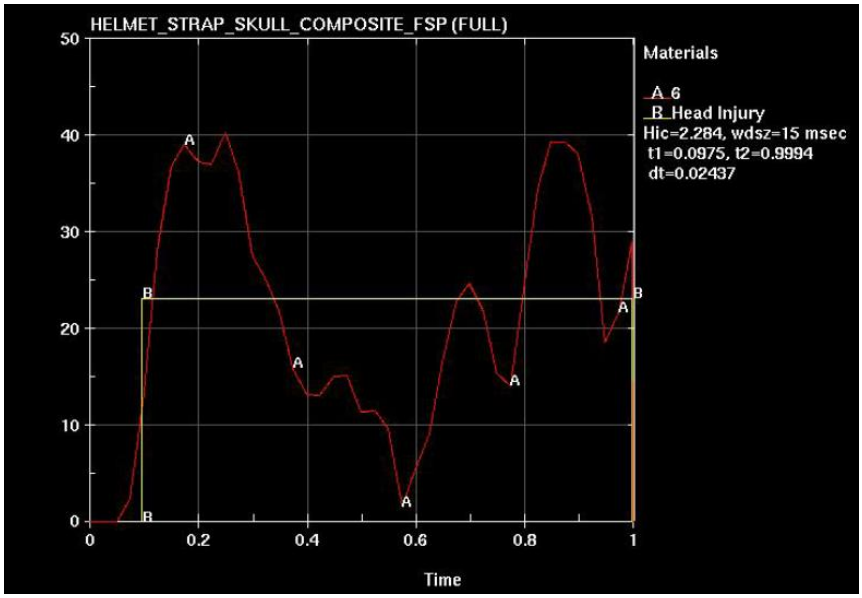

Figure7: HIC plot (frontal impact 90°)

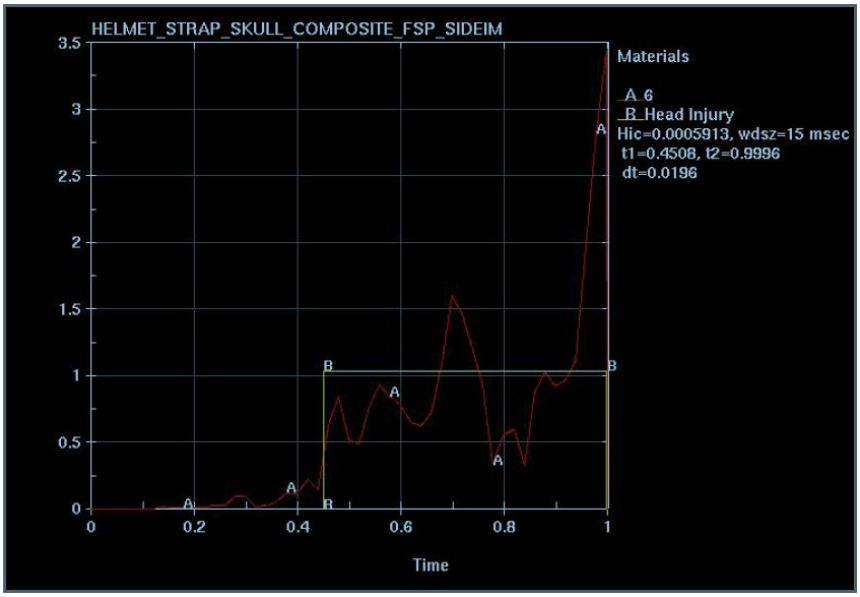

Figure 8: HIC plot (side impact 90°)

Discussion

A high fidelity head form model has been implemented in the ballistic impact simulation to a helmet in LS-DYNA environment. Various parameters have been investigated to better understand the ballistic helmet impact. HIC criterion has been used to assess the head injury. Simulation studies have shown that the both the impact angle and impact position have great effect on the HIC score. With a larger impact angle, the bullet will more likely skid over the surface of helmet and have less kinetic energy transferred to the helmet. When the bullet hits the back part of helmet, the largest HIC score, 54.52, has been observed compared to the situations when the bullet hits the other parts which are: 38.24 for the top; 24.40 for the front; 10.16 for the side. However, the HIC scores are not necessary to have the same trend as the values of Von Mises stress, maximum/minimum brain pressure or maximum principal strain in the brain because the HIC only depends on the resultant translational acceleration.

© Copyright 2014 | Centre for Info Bio Technology (CIBTech)

Different positions of human head have non-uniform thickness distribution and the thickest part is the forehead. Therefore, Von Mises stress, maximum/minimum brain pressure, and maximum principal strain in the brain are all the smallest when the helmet is impacted at the front part compared with the other three situations (Callahan, 2005).

Conclusion

The purpose of this project was (1) to study how different combat helmet shell stiffness affects the load levels in the human head during a bullet impact, and (2) to study how different impact angles affects the load levels in the human head. A detailed finite element (FE) model of the human head, in combination with an FE model of a combat helmet (the US Personal Armor System Ground Troops' (PASGT) geometry) was used. Focus was aimed on getting a realistic response of the coupling between the helmet and the head and not on modeling the helmet in detail. The studied data from the FE simulations were stress in the cranial bone, strain in the brain tissue, pressure in the brain, change in rotational velocity and translational and rotational acceleration. A parametric study was performed to see the influence of a variation in helmet shell stiffness on the outputs from the model. The effect of different impact angles was also studied. Dynamic helmet shell deflections larger than the initial distance between the shell and the skull should be avoided in order to protect the head from the most injurious threat levels. It is more likely that a fracture of the skull bone occurs if the inside of the helmet shell strikes the skull. Oblique ballistic impacts may in some cases cause higher strains in the brain tissue than pure radial ones.

REFERENCES

Aare M and Kleiven S (2007). Evaluation of head response to ballistic helmet impacts using the finite element method. *International Journal of Impact Engineering* **34**(3) 596–608.

Brands DWA (2002). *Predicting Brain Mechanics during Closed Head Impact: Numerical and Constitutive Aspects* (Proefschrift, University Press Facilities, Eindhoven, the Netherlands).

Callahan JE (2005). Analysis of Composite Helmet Impact by the Finite Element Method. PhD. Thesis, Faculty of the Virginia Polytechnic Institute and State University.

Gawande A (2004). Casualties of war--military care for the wounded from Iraq and Afghanistan. *The New England Journal of Medicine* **351**(24) 2471-5.

Helms G, Kallenberg K and Dechent P (2007). Contrast-driven approach to intracranial segmentation using a combination of T2- and T1-weighted 3D MRI data sets. *Journal of Magnetic Resonance Imaging* **24**(4) 790–795.

Hrapko M (2008). *Mechanical Behavior of Brain Tissue for Injury Prediction: Characterization and Modelling* (Proefschrift, University Press Facilities, Eindhoven, the Netherlands).

Prasad P and Mertz HJ (1985). The position of the United States delegation to the ISO working group on the use of HIC in the automotive environment. *SAE Paper 851246 Society of Automotive Engineers,* Warrendale PA, USA.

Sarron JC, Caillou JP, Da Cunha J, Allain JC and Tramecon A (2000). Consequences of nonpenetrating projectile impact on a protected head: study of rear effects of protections. *The Journal of Trauma* **49**(1) 923–9.

Van Hoof J, Cronin DS, Worswick MJ, Williams KV and Nandlall D (2001). Numerical head and composite helmet models to predict blunt trauma. In: *Proceedings of 19th International Symposium on Ballistics, Interlaken, Switzerland*.

Warden D (2008). Military TBI during the Iraq and Afghanistan wars. *The Journal of Head Trauma Rehabilitation* **21**(5) 398-402.

Zhang L, Yang KH and King AI (2004). A proposed injury threshold for mild traumatic brain injury. *Journal of Biomechanical Engineering* **126**(3) 226–236.

© Copyright 2014 | Centre for Info Bio Technology (CIBTech)